



ELSEVIER

Vibrational Spectroscopy 19 (1999) 143–149

VIBRATIONAL  
SPECTROSCOPY

## Set-up for time-resolved step-scan FTIR spectroscopy of noncyclic reactions

Robin Rammelsberg, Sophie Boulas, Harald Chorongiewski, Klaus Gerwert \*

*Lehrstuhl für Biophysik, Ruhr-Universität Bochum, 44780 Bochum, Germany*

Received 3 September 1998; revised 23 December 1998; accepted 4 January 1999

### Abstract

We have established a novel technique, which allows the application of time-resolved step-scan FTIR difference spectroscopy on noncyclic reactions. Cyclic reactions are ideally suited for the step-scan technique. However, it is difficult to apply the step-scan technique to noncyclic reactions, because the investigated process has to be repeated at about 1000 sampling positions of the interferogram. Consequently, to investigate noncyclic systems the sample has to be renewed at every sampling position. In the presented novel approach the IR-beam and the excitation laser-beam are focused to a very small diameter of 200  $\mu\text{m}$ . Thereby, only a small segment of the sample, which has an overall diameter of 15 mm, is excited and probed. By moving the sample, which is mounted on an x-y-stage, to different nonexcited segments the reaction can be repeated until a complete interferogram data set is recorded. In so far as the typically used flow cells are concerned their optical pathlength is too large to perform difference spectroscopy. We use 4  $\mu\text{m}$  thin films to depress the water background absorption of biological samples. As test, the well known photo-cyclic reactions of bacteriorhodopsin are measured. No systematic errors appear in the difference spectra. Because of intensity loss by the IR-microscope the signal-to-noise ratio is about 5 times less as compared to conventional step-scan measurements. For the first time, the technique is then applied to a noncyclic reaction, the photolysis of caged ATP. The successful performance with 10  $\mu\text{s}$  time-resolution now opens the door for many new applications of step-scan FTIR measurements to noncyclic reactions. © 1999 Elsevier Science B.V. All rights reserved.

**Keywords:** FTIR spectroscopy; Time-resolved; Noncyclic reactions

### 1. Introduction

Time-resolved step-scan FTIR difference spectroscopy has recently been established as a new tool to investigate reaction mechanisms of chemical and biological systems with atomic resolution [1–4]. The technique has been used to obtain vibrational spectra

of a variety of time-dependent systems. Examples are the determination of excited-state electronic structures [5,6], photo-acoustic measurements [7], studies of orientation dynamics in liquid-crystals [8], studies of polymer films [9], investigations of semiconductors [10], studies of C–H bond activation reactions [11], or determination of pericyclic reaction mechanisms [12]. Time-resolved step-scan FTIR spectroscopy is also established as a powerful new tool to investigate molecular reaction mechanisms of

\* Corresponding author. Tel.: +49-234-700-4461; Fax: +49-234-7094238; E-mail: gerwert@bph.ruhr-uni-bochum.de

proteins [13]. By performing difference spectra between a ground-state and a light activated state only absorbance bands of functionally active groups are selected. Complementary to structural resolving methods, like NMR- or X-ray, which provide static models of the protein ground-state, time-resolved FTIR difference spectroscopy monitors the activated states of proteins at atomic resolution. The proteins most intensively studied are the light-driven proton pump bacteriorhodopsin [14–16] and the light-induced electron transfer mechanism in photosynthetic bacterial reaction centers [17–20].

To perform time-resolved step-scan FTIR measurements, the movable mirror of the Michelson interferometer stops at every sampling position of the interferogram. At each position the reaction is started by a laser-flash and the time-course is recorded. In addition, it is usually necessary to average time-courses at every sampling position to improve the signal-to-noise ratio. Consequently, the investigated reaction has to be repeated usually more than  $1000 \times$  to yield a complete interferogram data set. Because of this restriction of time-resolved step-scan FTIR spectroscopy [21] almost all of the above mentioned applications are performed on cyclic or reversible reactions. Exceptions are described in Refs. [11,12], in which relatively large flow cells are used to exchange the sample between measurements at different sampling positions of the interferogram. However, a disadvantage of these flow cells is the large amount of sample needed. Furthermore, the demanded long optical pathway of about  $50 \mu\text{m}$  of flow cells decreases the transmission nearly to zero in the spectral region, where the solvent absorbs. Therefore, it is impossible to observe reliably the small absorbance changes in the order of  $10^{-3}$  in the spectral region of the solvent. Conventional flow cells cannot be used in our case.

Here, we present a novel approach to perform time-resolved step-scan FTIR measurements on non-cyclic reactions, by which absorbance changes in the order of  $1 \times 10^{-3}$  can be monitored in the entire IR spectral range with microsecond time-resolution. The time-resolution can easily be extended to the nanosecond time-range by using a faster IR-detector and a faster transient recorder. In addition, only very small amounts of sample ( $< 1 \mu\text{mol}$ ) are needed. In the past noncyclic reactions have usually been inves-

tigated with the rapid continuous-scan technique, which allows time-resolutions of about 10 ms [22–24].

This novel technique described here can be applied to a large variety of photobiological systems. It is also possible to measure reaction mechanisms of proteins without intrinsic chromophore by using photolabile trigger compounds now with microsecond time-resolution instead of millisecond time-resolution. With the use of caged GTP, the molecular GTPase mechanism of the oncogenic protein H-ras p21, a protein that plays a central role in the growth of cancer cells, can be monitored [25–27]. Another example is the  $\text{Ca}^{2+}$ -ATPase, which is triggered by caged  $\text{Ca}^{2+}$  [28,29]. Furthermore, 'caged' electrons can be used to study redox reactions in cytochrome-oxidases [30,31].

## 2. Experimental

The experimental set-up is shown in Fig. 1. The FTIR apparatus with IR-source (global) and Michelson interferometer is based on a BRUKER IFS66 spectrometer, which is equipped with an IR-microscope (BRUKER IRscope II) and an MCT-detector. The whole set-up, except for the excitation-laser, is positioned on a vibration isolation table (Newport) in a temperature-controlled laboratory.

The ac-coupled output of the detector-preamplifier system is digitized by a 12-bit, 200 kHz transient recorder (Keithley, AD-WIN 8). This transient recorder is connected to a PC. The PC also controls the sample positioning of the x-y-stage, triggers the laser-excitation and the stepping of the movable interferometer mirror.

The spectral range is limited below the Nyquist wavenumber  $1974 \text{ cm}^{-1}$  by an interference filter, which is positioned between sample and detector. This filter is not only used to reduce the number of sampling points of the interferogram but also to shield the detector from heat-radiation, which is emitted by the sample after laser-excitation.

Excitation of bacteriorhodopsin is achieved by an excimer pumped dye laser at 540 nm (Lambda Physik FL105 dye laser pumped by an LPX305i excimer laser). The photolysis reaction of caged ATP is started by a flash of a XeCl excimer laser at 308 nm

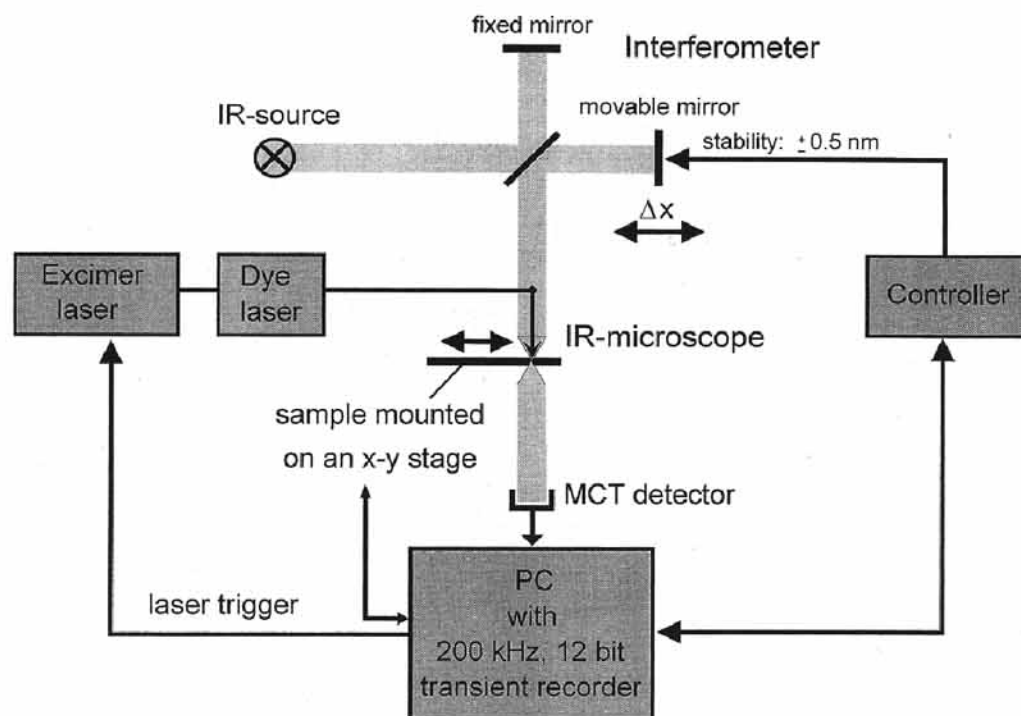


Fig. 1. Experimental set-up with IR-source, Michelson-interferometer, detector, transient recorder, and controller. The sample is mounted on a movable x-y-stage in the focus of an IR-microscope. An excimer pumped dye laser flash initiates the reaction.

(Lambda Physik LPX305i). The laser beam is focused to a spot of 200  $\mu\text{m}$  diameter on the sample using a telescope with an aperture. In order to avoid damage of the sample by the excitation-light the energy of the laser is restricted to less than 1 mJ per pulse. The pulse duration is 20 ns.

The sample, either a solution or in case of bacteriorhodopsin a suspension, is squeezed to a 4  $\mu\text{m}$  thin film between two  $\text{CaF}_2$  windows. The windows are specially polished to obtain very flat surfaces. One window has a sink of 4  $\mu\text{m}$  deepness and a diameter of 12 mm. This allows the preparation of very precise 4  $\mu\text{m}$  thin films, whose thickness varies less than  $\pm 10\%$  over the whole area.

The sample is mounted on a movable x-y-stage between the two Cassegrain-objectives of the microscope (Fig. 2). The IR-beam is focused to a diameter of 200  $\mu\text{m}$  overlapping optically with the excitation-laser. The movement of the stage is controlled by a PC and is correlated with the movement of the interferometer mirror.

Time-resolved measurements proceed as follows: the homogeneity of the sample is checked by measuring absorbance spectra at different positions of

the unphotolized sample. The deviations of the amplitudes of absorbance bands should be less than 10%.

The phase-spectrum is determined by recording an interferogram without moving the x-y-stage and without exciting the sample. The phase is stored and afterwards used for the Fourier transformation of the difference interferograms [4].

The sample area ( $\sim 2 \text{ cm}^2$ ) is divided into a few thousand segments with areas of 200  $\mu\text{m} \times 200 \mu\text{m}$  each. Typically, a sample consists of about 2000 segments. An interferogram has to have about 500 sampling positions to yield a spectrum between 950  $\text{cm}^{-1}$  and 1974  $\text{cm}^{-1}$  with a resolution of 8  $\text{cm}^{-1}$ . At each sampling position of the interferogram four time-courses can be averaged. Additional samples have to be used, if more coadditions should be made. This can be achieved by using a sample wheel.

The measurement is started by a laser-flash. The time-course of the IR-intensity at a specific sampling position is recorded. Then the next segment is moved into the focus of the laser- and IR-beam and the reaction is started again. After the measurement the collected time-courses of all sampling positions are

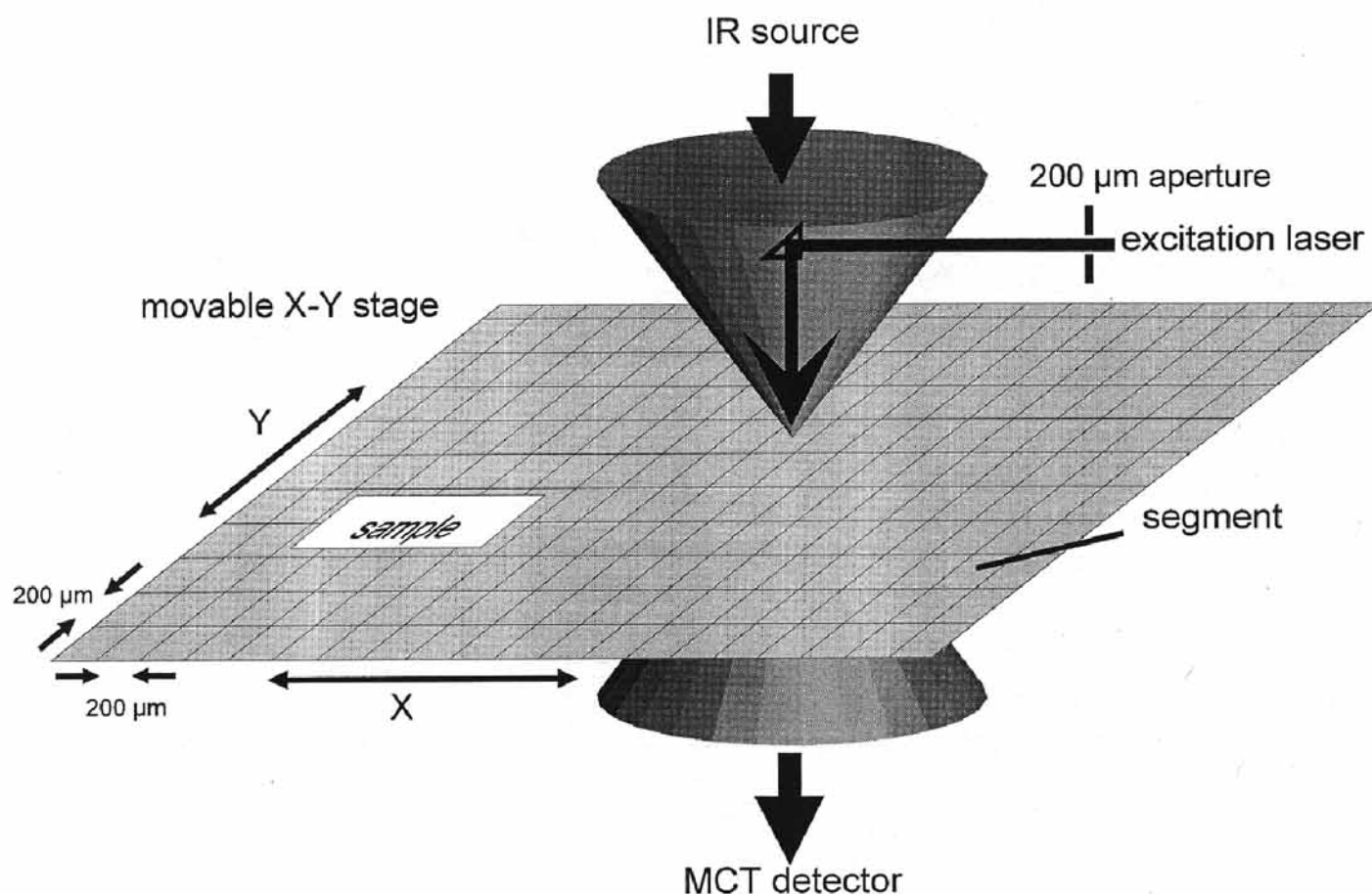


Fig. 2. The IR- and also the excitation laser-beam are focused to a diameter of 200  $\mu\text{m}$ . The sample is mounted on a movable x-y-stage and divided into a few thousand 200  $\mu\text{m} \times 200 \mu\text{m}$  segments. The reaction of the sample can be repeated by moving the next segment into the spot of the IR- and laser-beam.

rearranged to yield time-dependent interferograms [4].

### 2.1. Sample preparation

Bacteriorhodopsin is purified from *Halobacterium salinarum* as purple membrane sheets by a standard method [32]. It is suspended (200  $\mu\text{g}$  in 1 M KCl and 100 mM TRIS buffer at pH 7) and then centrifuged to concentrate the sample into a pellet. This pellet is squeezed between the two  $\text{CaF}_2$  windows.

**Caged ATP:** 40 mM caged ATP ( $\text{P}^3\text{-1-(2-nitro)phenylethyladenosin 5-triphosphate}$ , Molecular Probes), 150 mM MOPS buffer, pH 7, and 200 mM DTT (Dithiothreitol) are solved in 1  $\mu\text{l}$  water. This solution is squeezed between the two  $\text{CaF}_2$  windows.

The absorbance change  $\Delta A$  in the IR at the wave numbers  $\nu_i$  are analysed with sums of  $n_r$  exponen-

tials with apparent rate constants  $k_n$  and amplitudes  $a_n$ , where  $\{k_n\}$  is the same for all  $i$ .

$$\Delta A(\nu_i, t) = \sum_{n=1}^{n_r} a_n(\nu_i) e^{-k_n t}$$

For a detailed description, see Ref. [33].

### 3. Results and discussion

Time-resolved absorbance difference spectra of bacteriorhodopsin are compared in Fig. 3. The spectrum on top is measured in the conventional sample chamber of a Bruker IFS66 spectrometer as described in Ref. [16]. The bottom spectrum is measured with the novel technique. One hundred interferograms are averaged with a spectral resolution of 8  $\text{cm}^{-1}$  each. The difference is performed between spectra taken before and 100  $\mu\text{s}$  after laser excita-



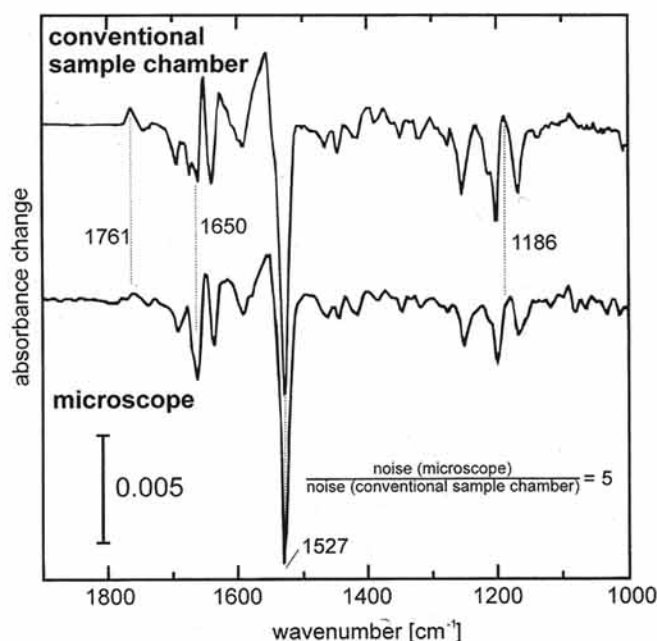


Fig. 3. Comparison of time-resolved step-scan FTIR difference absorbance spectra of bacteriorhodopsin measured in the conventional sample chamber (top) and in the microscope (bottom) of the Bruker IFS66 spectrometer. Both spectra are recorded 100  $\mu$ s after laser excitation with 8  $\text{cm}^{-1}$  spectral resolution.

tion. They represent differences between bacteriorhodopsin's ground-state and a mixture of the photointermediates L and M. (For details on bacteriorhodopsin see Ref. [33].) All typical bands are nicely resolved by the novel technique. For example, the 1761  $\text{cm}^{-1}$  band representing protonation of asp-85, the 1650  $\text{cm}^{-1}$  amid-I band, the 1527  $\text{cm}^{-1}$  retinal ethylene band, and the 1186  $\text{cm}^{-1}$  C–C retinal stretching vibration band can be observed. The comparison shows that systematic errors are below the noise level. However, the lower difference spectrum has increased noise as compared to the conventional measured difference spectrum. The differences between the two spectra, which are mostly observed in the amid-I region around 1650  $\text{cm}^{-1}$  and the fingerprint region around 1200  $\text{cm}^{-1}$ , are due to typical variations between different bR samples. We determine the noise of both spectra between 1800  $\text{cm}^{-1}$  and 1950  $\text{cm}^{-1}$  in a spectral region, where no specific bands appear. The root-mean-square of the noise in the spectrum measured by the microscope is  $4 \times 10^{-4}$ , which is only  $5 \times$  larger than in the conventional case. The results show that no systematic errors are introduced by the new approach.

In the next step the novel technique is applied to a noncyclic reaction, the photolysis of caged ATP (Fig. 4A). It is investigated with 10  $\mu$ s time-resolution and 15  $\text{cm}^{-1}$  spectral resolution. Caged ATP is a photolabile trigger compound [25]. It is used to initiate ATPase reactions by a light flash. In Fig. 4B time-resolved difference spectra of the caged ATP photolysis are shown. Five different samples of 1  $\text{cm}^2$  are used. The measurement of one sample takes about an hour. Ten interferograms are averaged in total. Controls show that the yield of the photolysis reaction decreases slightly during the measurement but not by more than 15%. This shows that the measurement at one segment is only little affected by scattered light of previous excitations. Furthermore, diffusion of the sample does not disturb the measurement.

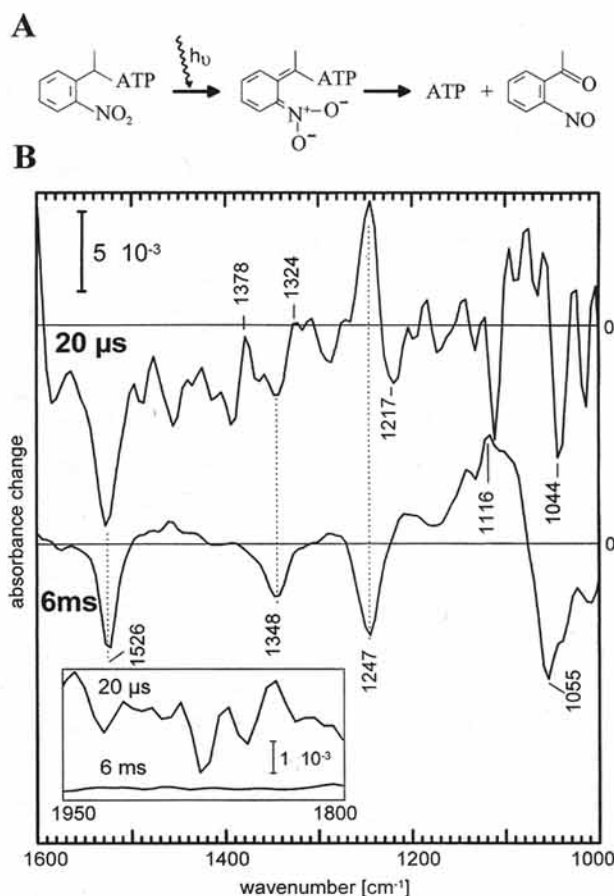


Fig. 4. Time-resolved difference absorbance spectra of the caged ATP photolysis, which are measured with the microscope. The 20  $\mu$ s spectrum (top) shows the *aci*-nitro intermediate. The 6 ms spectrum (bottom) shows free ATP and byproducts. In the insert the noise of the spectra are compared.

The spectrum shown at the top in Fig. 4B is taken 20  $\mu\text{s}$  after photo-excitation. It represents a difference spectrum between the initial state and the *aci*-nitro intermediate. The spectrum shows positive bands of the *aci*-nitro intermediate at 1378  $\text{cm}^{-1}$ , 1324  $\text{cm}^{-1}$ , and 1247  $\text{cm}^{-1}$  and negative bands of the initial state at 1526  $\text{cm}^{-1}$ , 1348  $\text{cm}^{-1}$ , 1217  $\text{cm}^{-1}$ , and 1044  $\text{cm}^{-1}$ . These bands agree nicely with low temperature spectra of caged ATP photolysis taken with rapid continuous-scan FTIR [25,34]. Only the negative band at 1044  $\text{cm}^{-1}$  is shifted about 15  $\text{cm}^{-1}$  to lower wave numbers compared to Ref. [34].

The difference spectrum taken 6 ms after photolysis shows free ATP and byproducts (Fig. 4B, bottom). The negative bands at 1526  $\text{cm}^{-1}$  of the asymmetric  $\text{NO}_2$  stretching vibration and at 1348  $\text{cm}^{-1}$  of the symmetric  $\text{NO}_2$  stretching vibration are still observed in this difference spectrum. At 1247  $\text{cm}^{-1}$  and 1116  $\text{cm}^{-1}$  new bands appear. The negative band, which is observed at 1044  $\text{cm}^{-1}$  in the 20  $\mu\text{s}$  spectrum, is shifted to 1055  $\text{cm}^{-1}$ . These features are also in nice agreement with Refs. [25,34].

The noise of the difference spectra is determined in the spectral range between 1800  $\text{cm}^{-1}$  and 1950  $\text{cm}^{-1}$  (Fig. 4B, insert), where no specific bands appear. The root-mean-square of the noise in the 20  $\mu\text{s}$  spectrum is  $1 \times 10^{-3}$ . This noise is mainly caused by the heat emission of the sample during the first 100  $\mu\text{s}$ . The heat emission is caused by laser excitation and decreases with a half-life of about 100  $\mu\text{s}$ . In the early time range, the amplitude of the heat emission has a larger amplitude than the IR intensity changes that are caused by absorbance changes of the sample. The time-course of the heat emission is the same at every sampling position of the interferogram. Therefore, it does not contribute to the difference spectra, except for increasing the noise [4]. After the disappearance of the heat emission the noise in the difference spectra also decreases. After 6 ms the signal-to-noise ratio is 10 times better as compared to 20  $\mu\text{s}$  (Fig. 4B, insert).

In order to show the capability to monitor kinetics of individual groups the time-resolved spectra are analysed by a global-fit [33]. The data are fitted by a sum of three exponentials with time-constants of 140  $\mu\text{s}$ , 3 ms, and 11 ms. The two faster time-constants describe the photolysis reaction, whereas the 11 ms

time-constant describes only the relaxation to zero, which is caused by the AC-coupling of the detector–preamplifier system.

As an example, the time-course of the 1247  $\text{cm}^{-1}$  band is shown in Fig. 5. It indicates the photolysis reaction. The band is caused by the  $\text{PO}_2$ -vibration at 1260  $\text{cm}^{-1}$  and the carbon–carbon-vibration of the  $\text{C}=\text{C}(\text{CH}_3)\text{O}$ -group at 1245  $\text{cm}^{-1}$  [26,34], which cannot be separated in our spectra due to the low spectral resolution of 15  $\text{cm}^{-1}$ . The positive absorbance band represents the *aci*-nitro intermediate. The appearance is not time-resolved, because it is much faster than the detector rise-time. The increase of the first few data points reflects the detector rise-time of about 10  $\mu\text{s}$ . Its disappearance and the formation of a negative band with the time-constants of 140  $\mu\text{s}$  and 3 ms indicates the decay of the *aci*-nitro intermediate to free ATP and byproducts.

In summary, the results of these two measurements show that the presented method allows the performance of time-resolved step-scan FTIR measurements of noncyclic reactions. Absorbance changes smaller than  $5 \times 10^{-3}$  are nicely resolved with a time resolution of 10  $\mu\text{s}$ . The time resolution can easily be expanded in the nanosecond range using a faster detector–amplifier system. Another advantage of the method is the small amount of

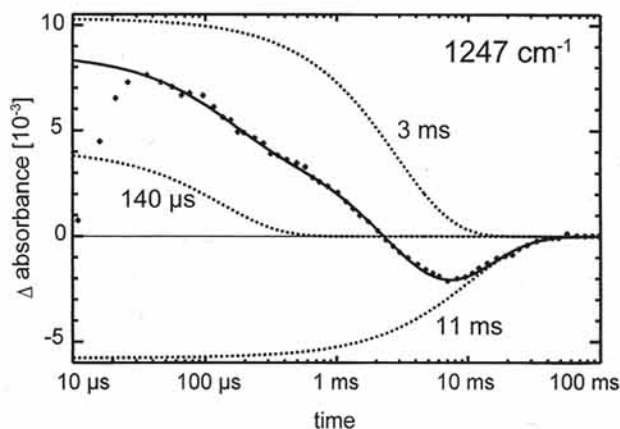


Fig. 5. The absorbance changes at 1247  $\text{cm}^{-1}$  are shown as an indicator of the photolysis reaction of caged ATP. The three dotted exponentials compose the fitted curve (continuous line). The exponentials with time-constants of 140  $\mu\text{s}$  and 3 ms describe a biphasic transition from the *aci*-nitro intermediate to free ATP and byproducts. The exponential with a time-constant of 11 ms is a result of the AC-coupling of the detector preamplifier, which causes a relaxation of all signals to zero.

sample needed. In the case of the caged ATP measurement 0.2  $\mu\text{mol}$  caged ATP are used.

Many applications of this technique in photochemistry are now feasible. Examples are photopolymerizations, photoisomerizations, or photodissoziations.

## Acknowledgements

This work was supported by the Deutsche Forschungsgemeinschaft, SFB 394, Teilprojekt C2. The time-resolved FTIR step-up and the x-y-stage set-up (patent pending #198 04 279.5-52) is commercially available (E-mail: gerwert@bph.ruhr-uni-bochum.de; Fax: +49-251-270-4229).

## References

- [1] R.A. Palmer, C.J. Manning, J.L. Chao, I. Noda, A.E. Dowrey, C. Marcott, *Appl. Spectrosc.* 45 (1991) 12.
- [2] W. Uhmann, A. Becker, C. Taran, F. Siebert, *Appl. Spectrosc.* 45 (1991) 390.
- [3] R.A. Palmer, J.L. Chao, R.M. Dittmar, V.G. Gregoriou, S.E. Plunkett, *Appl. Spectrosc.* 47 (1993) 1297.
- [4] R. Rammelsberg, B. Heßling, H. Chorongiewski, K. Gerwert, *Appl. Spectrosc.* 51 (1997) 558.
- [5] P.Y. Chen, R.A. Palmer, *Appl. Spectrosc.* 51 (1997) 580.
- [6] J.R. Schoonover, G.F. Strouse, R.B. Dyer, W.D. Bates, P.Y. Chen, T.J. Meyer, *Inorg. Chem.* 35 (1996) 273.
- [7] E.Y. Jiang, R.A. Palmer, N.E. Barr, N. Morosoff, *Appl. Spectrosc.* 51 (1997) 1238.
- [8] M.A. Czarnecki, S. Okretic, H.W. Siesler, *J. Phys. Chem. B.* 101 (1997) 374.
- [9] H.C. Wang, R.A. Palmer, C.J. Manning, *Appl. Spectrosc.* 51 (1997) 1245.
- [10] W. Hilber, M. Helm, K. Alavi, R.N. Pathak, *Appl. Phys. Lett.* 69 (1996) 2528.
- [11] S.E. Bromberg, H. Yang, M.C. Asplund, T. Lian, B.K. McNamara, K.T. Kotz, J.S. Yeston, M. Wilkens, H. Frei, R.G. Bergman, C.B. Harris, *Science* 278 (1997) 260.
- [12] E. Kauffmann, H. Frei, R.A. Mathies, *Chem. Phys. Lett.* 266 (1997) 554.
- [13] K. Gerwert, *Current Opinion Structural Biology* 3 (1993) 769.
- [14] O. Weidlich, F. Siebert, *Appl. Spectrosc.* 47 (1993) 1394.
- [15] B. Heßling, J. Herbst, R. Rammelsberg, K. Gerwert, *Biophys. J.* 73 (1997) 2071.
- [16] R. Rammelsberg, G. Huhn, M. Lübben, K. Gerwert, *Biochemistry* 35 (1998) 5001.
- [17] J.-R. Burie, W. Leibl, E. Navedryk, J. Breton, *Appl. Spectrosc.* 47 (1993) 140.
- [18] K. Gerwert, B. Hess, H. Michel, S. Buchanan, *FEBS Lett.* 232 (1988) 303.
- [19] R. Brudler, K. Gerwert, *Photosynthesis Research* 55 (1998) 261.
- [20] R. Brudler, H.J.M. de Groot, W.B.S. van Liemt, W.F. Steggerda, R. Esmeijer, P. Gast, A.J. Hoff, J. Lugtenburg, K. Gerwert, *EMBO J.* 13 (1994) 5523.
- [21] J.J. Turner, M.W. George, M. Poliakoff, *Spec. Publ. R. Chem.* 163 (1995) 13.
- [22] M.S. Braiman, P.L. Ahl, K.J. Rothschild, *Proc. Natl. Acad. Sci. USA* 84 (1987) 5221.
- [23] K. Gerwert, *Ber. Bunsenges. Phys. Chem.* 92 (1988) 978.
- [24] K. Gerwert, G. Souvignier, B. Hess, *Proc. Natl. Acad. Sci. USA* 87 (1990) 9774.
- [25] V. Cepus, C. Ulbrich, C. Allin, A. Troullier, K. Gerwert, *Methods Enzymol.* 291 (1998) 223.
- [26] K. Gerwert, V. Cepus, A. Scheidig, R.S. Goody, in: A. Lau, F. Siebert, W. Werncke (Eds.), *Time Resolved Vibrational Spectroscopy*, Springer Verlag, Berlin, 1994, p. 256.
- [27] V. Cepus, A.J. Scheidig, R.S. Goody, K. Gerwert, *Biochemistry* 37 (1998) 10263.
- [28] A. Barth, W. Kreutz, W. Mäntele, *Biochim. Biophys. Acta* 1057 (1991) 115.
- [29] A. Troullier, K. Gerwert, Y. Dupont, *Biophys. J.* 71 (1996) 2970.
- [30] M. Lübben, K. Gerwert, *FEBS Lett.* 397 (1996) 303.
- [31] M. Lübben, A. Prutsch, B. Mamat, K. Gerwert, *Electron transfer induces side chain conformational changes of Glu-286 from cytochrom  $b_0$ , Biochemistry*, in press.
- [32] D. Oesterhelt, W. Stoekenius, *Methods Enzymol.* 31 (1974) 667.
- [33] B. Heßling, G. Souvignier, K. Gerwert, *Biophys. J.* 65 (1993) 1929.
- [34] A. Barth, J.E.T. Corrie, M.J. Gradwell, Y. Maeda, W. Mäntele, T. Meier, D.R. Trentham, *J. Am. Chem. Soc.* 119 (1997) 4149.